

Molecular Recognition of Ubiquinone Analogues. Specific Interaction between Quinone and Functional Porphyrin via Multiple Hydrogen Bonds

Takashi Hayashi,^{*,†} Takashi Miyahara,[†] Norihiro Koide,[†] Yukitoshi Kato,[†] Hideki Masuda,[‡] and Hisanobu Ogoshi^{*,†,§}

Contribution from the Department of Synthetic Chemistry and Biological Chemistry, Graduate School of Engineering, Kyoto University, Kyoto 606-01, Japan, and Department of Applied Chemistry, Nagoya Institute of Technology, Nagoya 466, Japan

Received April 10, 1997[⊗]

Abstract: *meso*- $\alpha,\alpha,\alpha,\alpha$ -Tetrakis(2-hydroxy-1-naphthyl)porphyrin (**1**) and 5,15-*cis*-bis(2-hydroxy-1-naphthyl)-10,20-diphenylporphyrin (**2**) were prepared as receptors for ubiquinone analogues. UV-vis, IR, NMR, and X-ray crystal data reveal that these porphyrins bind a series of quinones with a cofacial structure linked by hydrogen bonds. The binding constants of **1** for quinones increase with the number of MeO substituents bound to a quinone ring. Compared to 2,5-dimethoxy-*p*-benzoquinone, 2,3-dimethoxy-*p*-benzoquinone shows more favorable negative changes in ΔG° and ΔH° upon binding with **1**, whereas the interaction between **2** and quinone is not affected by the position and number of MeO substituents. Thus the two adjacent MeO substituents cooperatively act as the third recognition site for OH groups in **1** to form the bifurcated hydrogen bonding. Particularly, tetramethoxy-*p*-benzoquinone (**4f**) shows an extremely large affinity and favorable ΔH° with **1** due to the formation of simultaneous multiple hydrogen bonds; $\Delta G^\circ = -7.9$ kcal/mol at 298 K in toluene. The van't Hoff plots obtained from titrimetric measurement at 0.9–5.2 mol % ethanol in toluene reveal a nonlinear relationship between $R \ln K$ and $1/T$. The curvature of these plots is explained in terms of the temperature dependence of the degree of functional groups solvation in **1** and **4f** with a negative heat capacity change; $\Delta C_p^\circ = -5.6 \times 10^2$ cal/mol·K at 0.9 mol % ethanol, indicating that the solvent–solute interaction has a crucial effect on the stability of the host–guest complexes.

Introduction

Molecular recognition and molecular assembly in protein–ligand binding quite often dominate the protein functions such as highly specific recognition manner, catalytic reaction, transportation, regulation, and so on. In these processes, thermodynamic parameters for host–guest complexation give us significant information about the mechanism of efficient binding.¹ However, the overall thermodynamic changes of host–guest complexation in biological systems are the net result of many kinds of weak interactions and are generally quite complicated. Therefore, one of the current research efforts in our laboratory addresses the artificial host–guest complexation formed by noncovalent weak interactions, such as hydrogen bonds and salt bridges as well as hydrophobic contacts, to elucidate the thermodynamic and kinetic mechanisms of molecular recognition in biological systems.

In the last decade, a number of model studies on structural features of intermolecular interactions and the thermodynamic parameters in molecular recognition events have been reported in the literature, some of them giving a deep insight into the mechanism of complexation.^{2,3} We and several other groups have demonstrated that synthetic porphyrins having some

functional sites are quite suitable host molecules for small biomolecular guests.⁴ Our reasons for choosing porphyrin units for investigation of host–guest complexation are 3-fold: (i) The porphyrin unit is a rigid and flat enough framework for the design of a host molecule preorganized for a guest structure. (ii) Various functional groups are easily fixed at *meso* and peripheral β -pyrrole positions on the porphyrin ring. (iii) The physical properties and structural features of host–guest interactions are readily monitored by several convenient spectroscopic measurements due to the characteristic aromaticity of the porphyrin ring. Therefore, in a series of artificial host molecules, porphyrin units are widely used as molecular platforms.

Recently, we have focused our attention on the elucidation of the interaction between enzyme and ubiquinone which works as an electron or proton carrier in the mitochondrial respiratory chain. The ubiquinone has a long isoprenoid tail and two adjacent MeO substituents bound to the ring of *p*-benzoquinone and is freely movable to carry the electron or proton to the oxidoreductases in the mitochondrial lipid layer.^{5,6} Therefore, it is of particular interest to design a new type of ubiquinone receptor by use of a porphyrin framework, since electron transfer (ET) between porphyrin and quinone components is one of the most current topics in chemistry and biology.⁷ However, the model study on the noncovalently linked porphyrin–quinone complex has been quite limited.⁸ Recently, we have studied the specific intermolecular interaction between ubiquinone and

[†] Kyoto University.

[‡] Nagoya Institute of Technology.

[§] Current address: Fukui National College of Technology, Geshi, Sabae 916, Japan.

[⊗] Abstract published in *Advance ACS Abstracts*, July 15, 1997.

(1) (a) Lumry, R.; Rajender, S. *Biopolymers* **1970**, *9*, 1125. (b) Eftink, M.; Biltonen, R. In *Biological Microcalorimetry*; Beezer, A. E., Ed.; Academic Press: New York, 1980; pp 343–412. (c) Alvarez, J.; Biltonen, R. *Biopolymers* **1973**, *12*, 1815.

(2) For recent reviews: Hamilton, A. D., Ed.; *Molecular Recognition* (Tetrahedron Symposia No. 56). *Tetrahedron* **1995**, *51*.

(3) Lehn, J.-M. *Supramolecular Chemistry*; VCH: Weinheim, 1995.

(4) For example: (a) Ogoshi, H.; Kuroda, Y.; Mizutani, T.; Hayashi, T. *Pure Appl. Chem.* **1996**, *68*, 1411. (b) Ogoshi, H.; Mizutani, T. In *Comprehensive Supramolecular Chemistry*; Murakami, Y., Ed.; Oxford, 1996; Vol. 4; p 337.

(5) Gennis, R. B. *Biomembranes*; Springer-Verlag: New York, 1989.

(6) (a) Crane, F. L. *Ann. Rev. Biochem.* **1977**, *46*, 439. (b) Hackenbrock, C. R.; Chazotte, B.; Gupta, S. S. *J. Bioenerg. Biomembr.* **1986**, *18*, 331.

(c) Lenaz, G.; Fato, R. *J. Bioenerg. Biomembr.* **1986**, *18*, 369.

the porphyrin *meso*- $\alpha,\alpha,\alpha,\alpha$ -tetrakis(2-hydroxy-1-naphthyl)-porphyrin (**1**), which has four convergent OH groups as functional sites above the plane of the porphyrin ring.⁹ Furthermore, we have reported that the porphyrin π -cation radical species as an intermediate of photoinduced ET process has been directly detected in the specific noncovalent adduct of zinc complex of **1** and quinone.¹⁰

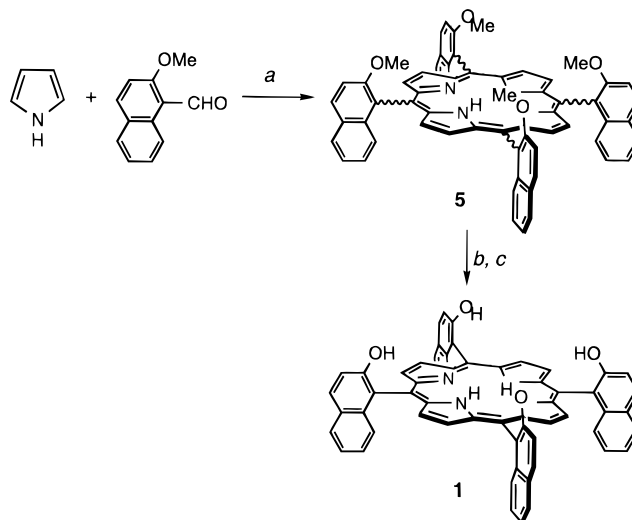
On the other hand, we found that the solvation/desolvation of functional groups associated with a hydrogen-bonded site dramatically influences the thermodynamic behavior of the porphyrin–quinone complexation accompanied by a large negative heat-capacity change (ΔC_p°) due to the temperature-dependent solvation in toluene–ethanol binary solvent. To our knowledge, few definitive works concerning the thermodynamic aspects of host–guest complex via hydrogen-bonding interactions have been carried out in the presence of polar solvents,^{11,12} although hydrogen bonding between the protein and the ligand is one of the most essential interactions in promoting a binding process in an enzyme pocket.

In this paper, we report the characterization of the porphyrin–quinone adduct in solution and solid states and discuss the thermodynamic parameters for complexation in toluene. The obtained results indicate that (i) the two adjacent MeO groups play an important role in the specific binding of ubiquinone analogues by multifunctional porphyrin host **1** and (ii) the complexation in toluene–ethanol binary solvent reveals the solvent effect on the thermodynamic parameters with a large negative ΔC_p° . This study examines the fundamental influence of solvation in protein–ligand complexation in the presence of water in biological systems. In addition, we wish to present that this system can be regarded as a model for the subunits of complex **I** and **III** which might have a specific binding site for ubiquinone electron acceptor in the respiratory system.¹³

Results and Discussion

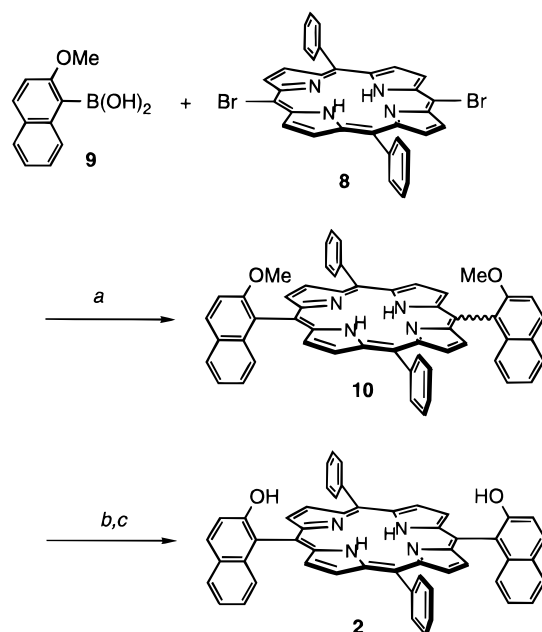
Preparation of Porphyrin Host Molecules. Porphyrin **1** was prepared by condensation of pyrrole and 2-methoxy-1-naphthaldehyde, followed by deprotection of the four methyl groups of **5** by BBr_3 as shown in Scheme 1. The obtained porphyrin comprises four atropisomers and the desired $\alpha,\alpha,\alpha,\alpha$ -atropisomer was readily separated by silica gel column chromatography ($R_f = 0.24$, benzene–ethyl acetate = 1:1). Furthermore, atropisomerization due to the rotation about carbon

Scheme 1^a



^a (a) $\text{BF}_3\text{OEt}_2/\text{DDQ}/\text{EtOH}/\text{benzene}$, (b) $\text{BBr}_3/\text{CH}_2\text{Cl}_2$, (c) silica gel column chromatography.

Scheme 2^a



^a (a) $\text{Pd}(\text{PPh}_3)_4/\text{Na}_2\text{CO}_3/\text{benzene}$, (b) $\text{BBr}_3/\text{CH}_2\text{Cl}_2$, (c) separation of *cis* and *trans* isomers by silica gel column chromatography.

(*meso*)–carbon (naphthyl) bonds was not detected even in boiling toluene over 2 h.¹⁴

Porphyrin **2** possessing two 2-hydroxynaphthyl groups was designed as a reference host molecule. Since one-step synthesis by condensation of benzaldehyde, 2-methoxy-1-naphthaldehyde, and pyrrole (1:1:2) afforded a mixture of geometric isomers, porphyrin **2** was prepared by stepwise synthesis as shown in Scheme 2. The precursor, 5,15-diphenylporphyrin (**7**), was prepared by condensation of dipyrromethane (**6**) and benzaldehyde in the presence of CF_3COOH and sequential oxidation by DDQ.¹⁵ The brominated compound, 5,15-dibromo-10,20-diphenylporphyrin (**8**), was easily available from the treatment of a chloroform solution of porphyrin **7** with 2 equiv of *N*-bromosuccinimide.^{16,17b}

(7) For recent reviews on ET reactions by covalently or noncovalently linked porphyrin–quinone compounds: (a) Wasielewski, M. R. *Chem. Rev.* **1992**, 92, 435. (b) Sessler, J. L. *Isr. J. Chem.* **1992**, 32, 449. (c) Kurreck, H.; Huber, M. *Angew. Chem., Int. Ed. Engl.* **1995**, 34, 849. (d) Sessler, J. L.; Wang, B.; Springs, S. L.; Brown, C. T. In *Comprehensive Supramolecular Chemistry*, Vol. 4; Murakami, Y., Ed.; Oxford, 1996; p 311.

(8) (a) Aoyama, Y.; Asakawa, M.; Matsui, Y.; Ogoshi, H. *J. Am. Chem. Soc.* **1991**, 113, 6233. (b) Harriman, A.; Kubo, Y.; Sessler, J. L. *J. Am. Chem. Soc.* **1992**, 114, 388. (c) Kuroda, Y.; Ito, M.; Sera, T.; Ogoshi, H. *J. Am. Chem. Soc.* **1993**, 115, 12210. (d) Sessler, J. L.; Wang, B.; Harriman, A. *J. Am. Chem. Soc.* **1993**, 115, 10418. (e) Berman, A.; Izraeli, E. S.; Levanon, H.; Wang, B.; Sessler, J. L. *J. Am. Chem. Soc.* **1995**, 117, 8252. (f) D'Souza, F. J. *Am. Chem. Soc.* **1996**, 118, 923. (g) Hunter, C. A.; Shannon, R. J. *Chem. Commun.* **1996**, 1361.

(9) (a) Hayashi, T.; Miyahara, T.; Hashizume, N.; Ogoshi, H. *J. Am. Chem. Soc.* **1993**, 115, 2049. (b) Hayashi, T.; Asai, T.; Hokazono, H.; Ogoshi, H. *J. Am. Chem. Soc.* **1993**, 115, 12210. (c) Hayashi, T.; Miyahara, T.; Aoyama, Y.; Kobayashi, M.; Ogoshi, H. *Pure Appl. Chem.* **1994**, 66, 797. (d) Hayashi, T.; Miyahara, T.; Aoyama, Y.; Nonoguchi, M.; Ogoshi, H. *Chem. Lett.* **1994**, 1749.

(10) Hayashi, T.; Miyahara, T.; Kumazaki, S.; Yoshihara, K.; Ogoshi, H. *Angew. Chem. Int. Ed. Engl.* **1996**, 35, 1964.

(11) Bonar-Law, R. P.; Sanders, J. K. M. *J. Am. Chem. Soc.* **1995**, 117, 259.

(12) Adrian, J. C. Jr.; Wilcox, C. S. *J. Am. Chem. Soc.*, **1991**, 113, 678.

(13) (a) Trumpower, B. L. *J. Biol. Chem.* **1990**, 265, 11409. (b) Hofhaus, G.; Weiss, H.; Leonard, K. *J. Mol. Biol.* **1991**, 221, 1027.

(14) Gottwald, L. K.; Ullman, E. F. *Tetrahedron Lett.* **1969**, 3071.

(15) Manka, J. S.; Lawrence, D. S. *Tetrahedron Lett.* **1989**, 30, 6989.

(16) Nudy, L. R.; Hutchinson, H. G.; Schieber, C.; Longo, F. R. *Tetrahedron* **1984**, 40, 2359.

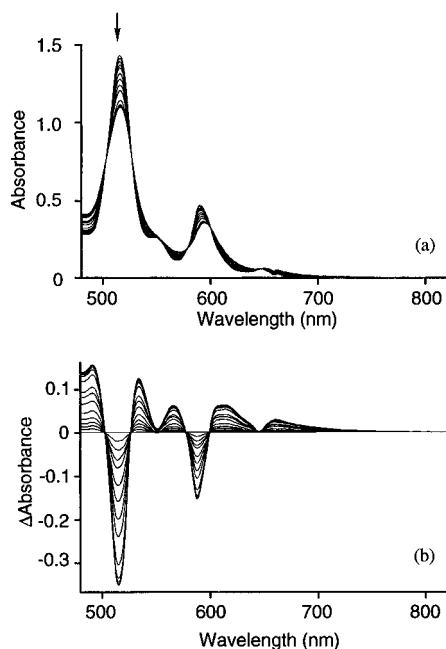


Figure 1. (a) Visible spectrum of **1** ($[1]_0 = 7.3 \times 10^{-5}$ M) in the presence of various amounts of **4f** ($[4f]_0 = 0-1.8 \times 10^{-4}$ M) in toluene at 298 K. (b) Difference spectra of spectrum a.

Carbon-carbon bond formation between the porphyrin ring and a variety of aryl and allyl groups by metal-mediated cross-coupling is a versatile method to prepare new functional porphyrins. Recently, Therien et al. have reported a new approach for the catalytic reaction of bromoporphyrin and aryl halide in the presence of palladium catalyst.¹⁷ In our case, the desired substituted porphyrin **10** was not obtainable from any combinations of the zinc complex of **8** and organometallic species (RZnX or RMgX) generated from 1-bromo-2-methoxynaphthalene in the presence of Pd(0) or Ni(0) catalyst. In this case, the cross-coupling reaction of porphyrin **8** and (2-methoxy-1-naphthaleneboronic acid (**9**) in the presence of Na_2CO_3 and $\text{Pd}(\text{PPh}_3)_4$ in benzene^{18,19} gave 5,15-bis(2-methoxy-1-naphthyl)-10,20-diphenylporphyrin (**10**) in 20% yield (a mixture of *cis* and *trans* isomers). After deprotection of two methyl groups by BBr_3 , the desired *cis* isomer **2** was readily obtained by silica gel column chromatography.

Intermolecular Interaction between Porphyrin and Quinone. Binding events of host porphyrin **1** and **2** for a series of quinones were monitored by UV-vis spectroscopic titration, as shown in Figure 1. The Q-band of each porphyrin in the range of 500–700 nm drastically changed with observation of several isosbestic points upon addition of quinone, and a Job's plot gave a maximum at 0.5 mole ratio. These spectral changes support the 1:1 complexation between porphyrin and quinone.

The IR spectra for **1**, tetramethoxy-*p*-benzoquinone (**4f**), and a mixture of **1** and **4f** were measured in CHCl_3 at room temperature. Addition of quinone **4f** decreased the OH stretching vibration of **1** at 3544 cm^{-1} and increased a new absorption band at 3449 cm^{-1} . The lower frequency broad band is assigned to the OH groups interacting with **4f** via hydrogen bonding. At a 1:1 ratio of **1** and **4f**, the free OH band at 3544 cm^{-1} almost disappeared. A mixture of **2** and **4f** showed two bands at 3546 cm^{-1} for the free OH stretching vibration and at 3452 cm^{-1}

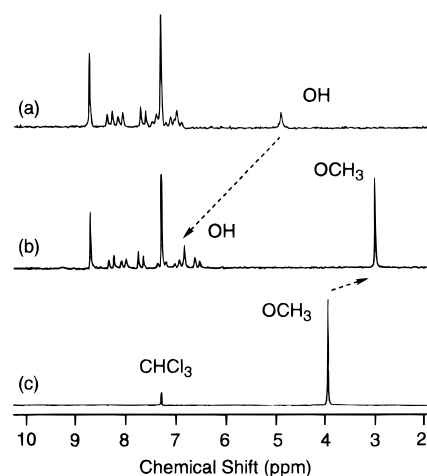


Figure 2. ^1H NMR spectrum (90 MHz) of (a) **1** ($[1] = 2.03 \times 10^{-3}$ M), (b) a mixture of **1** ($[1]_0 = 1.73 \times 10^{-3}$ M) and **4f** ($[4f]_0 = 1.71 \times 10^{-3}$ M), and (c) **4f** ($[4f] = 1.13 \times 10^{-2}$ M) in CDCl_3 at 303 K.

due to the hydrogen-bonded OH band. These spectra demonstrate that the porphyrin-quinone complex is linked by hydrogen bonding.

Figure 2 shows the prominent NMR spectra for the **1**·**4f** complex. Addition of 1 equiv of **4f** to a CDCl_3 solution of **1** gave characteristic changes in the chemical shifts of OH protons in **1** and MeO protons in **4f**. Large downfield shift of OH protons from 4.90 to 6.81 ppm ($\Delta\delta = 1.91$ ppm) demonstrates that the hydrogen-bonding interaction between porphyrin and quinone is through OH groups.²⁰ The MeO protons in **4f** shifted to upfield ($\Delta\delta = -0.94$ ppm) due to the diamagnetic ring current of the aromatic host **1**. The spectrum of a 1:1 mixture of **1** and 2,3,5-trimethoxy-*p*-benzoquinone (**4e**) also revealed the large upfield shift of olefinic proton resonance of **4e** ($\Delta\delta = -1.14$ ppm). Similar shifts are found in the titration study of quinones to **2** in CDCl_3 and toluene- d_8 . These results support the cofacial structure of porphyrin-quinone complex.

Determination of Porphyrin-Quinone Complex in the Solid-State. An X-ray structural study was conducted on a single crystal of the **1**·**4f** pair obtained from CHCl_3 , and the molecular structures are depicted in Figure 3 with the numbering scheme of the N and O atoms. The unit cell contains six **1**·**4f** pairs at 1:1 stoichiometry and eight solvated chloroform molecules. The crystallographically independent porphyrin complexes in the unit cell are one (Figure 3a) and a half (see Supporting Information) molecules, in which the latter half molecule is completed by the relation of a 2-fold axis in the center of the porphyrin. As expected from several spectroscopies, all four hydroxynaphthyl groups attached to *meso*-positions of **1** are oriented upward, and the porphyrin rings, which are planar within 0.10 and 0.12 Å,²¹ form noncovalent face-to-face stacking with **4f** with the separation distances of

(20) Binding constants can be determined from changes in chemical shift of OH groups by titration of a quinone solution with a CDCl_3 solution of **1**. The binding constants of **4a**, **4d**, and **4f** at 298 K are determined from the downfield shifts of OH signals; $K_{a(4a)} = 1.5 \times 10^2$, $K_{a(4d)} = 7.5 \times 10^2$, and $K_{a(4f)} = 5.6 \times 10^4\text{ M}^{-1}$, respectively, whereas same binding constants determined from UV-vis titration in CHCl_3 at 298 K are 3.0×10^2 , 8.3×10^2 , and $2.0 \times 10^4\text{ M}^{-1}$, respectively.^{9a} The binding constant determined from the NMR titrimetric measurement is exactly consistent with that from the UV-vis titrimetric one.

(21) The detected planarity of porphyrin ring suggests that the remarkable structural changes upon complexation between **1** and **4f** does not occur. Thus, the structure of **1** seems to be preorganized for ubiquinone analogues. The planarity of the porphyrin ring in tetraphenylporphyrin has been reported previously. For example: (a) Hamor, M. J.; Hamor, T. A.; Hoard, J. L. *J. Am. Chem. Soc.* **1964**, *86*, 1983. (b) Senge, M. O.; Forsyth, T. P.; Nguyen, L. T.; Smith, K. M. *Angew. Chem. Int. Ed. Engl.* **1994**, *33*, 2485.

(17) (a) DiMaggio, S. G.; Lin, V. S.-Y.; Therien, M. J. *J. Am. Chem. Soc.* **1993**, *115*, 2513. (b) DiMaggio, S. G.; Lin, V. S.-Y.; Therien, M. J. *J. Org. Chem.* **1993**, *58*, 5983.

(18) (a) Miyaura, N.; Yanagi, T.; Suzuki, A. *Synth. Commun.* **1981**, *11*, 513. (b) Suzuki, A. *Pure Appl. Chem.* **1994**, *66*, 213.

(19) Zhou, X.; Chan, K. S. *J. Chem. Soc., Chem. Commun.* **1994**, 2493.

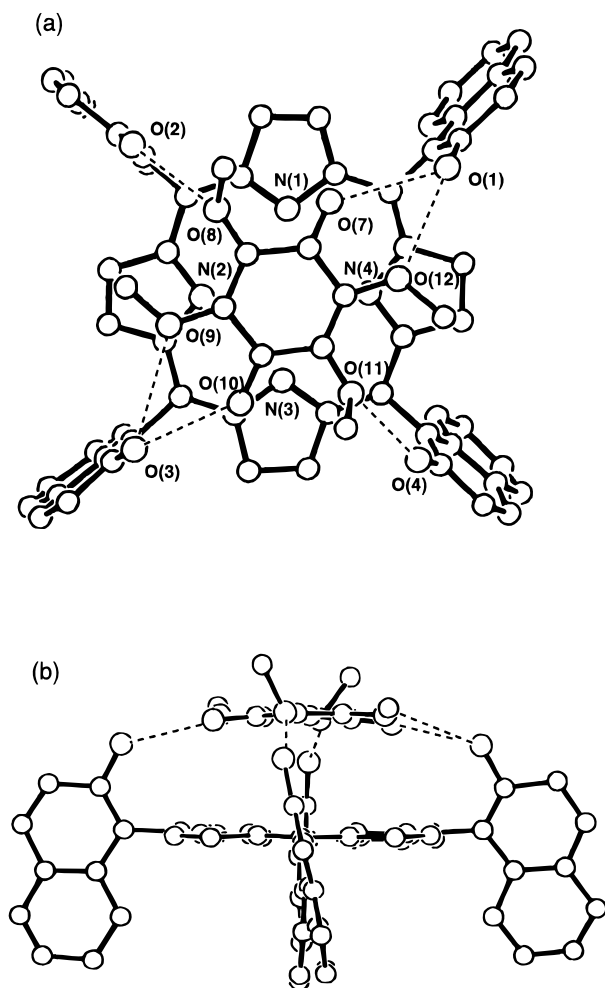


Figure 3. X-ray crystal structure of **1·4f** complex. The solvent molecules are omitted for clarity: (a) top view of one molecular structure and (b) side view for one molecular structure.

3.35 and 3.35 Å, which agree with van der Waals distance between aromatic rings (3.4 Å). Also four OH groups form hydrogen bonds with two carbonyl oxygens and four MeO oxygens of **4f** [(O(1)···O(7) = 2.98, O(1)···O(12) = 3.01, O(2)···O(8) = 2.86, O(3)···O(9) = 3.3, O(3)···O(10) = 2.84, O(4)···O(11) = 2.69, O(5)···O(14) = 2.87, O(5)···O(15) = 3.18, O(6)···O(13) = 2.86 Å], as shown in Figure 3. The direction of the carbonyl oxygen lone pairs that lie on the same plane as the quinone ring in **4f** could require the orientation of the hydrogen bonding. Furthermore, two of four MeO groups in **4f** are oriented upward to avoid steric hindrance with porphyrin molecules and the other two MeO groups are located on the same plane as the quinone ring to accept acidic OH groups which also interact with the carbonyl oxygen.²² Therefore, quinone molecules rotate about a temporary 4-fold axis on the porphyrin ring with twisting angles of 12° and 12° to form the complementary hydrogen bonding network with **1**.

Binding Affinities and Thermodynamic Parameters of Porphyrin–Quinone Complexation. Binding constants, K_a , and thermodynamic parameters, ΔG° , ΔH° , and $T\Delta S^\circ$, in toluene at 298 K are summarized in Tables 1 and 2. The enthalpy and entropy changes were calculated from the slope and intercept of van't Hoff plots, which show a linear relation-

ship between $1/T$ and $\ln K_a$ in the range of 288–328 K. Table 1 presents the relationship between the thermodynamic parameters and the number of MeO substituents bound to the ring of *p*-benzoquinone. The ΔG° , ΔH° , and ΔS° values for complexation between **1** and **4a–f** negatively increase with the number of MeO groups. Particularly, the differential free energy changes, $\Delta\Delta G^\circ$,²³ represent the binding mode of quinones. When we focus on the difference in the number of MeO substitutions in quinones **4a–f**, the $\Delta\Delta G^\circ_{1.4b-1.4a}$, $\Delta\Delta G^\circ_{1.4c-1.4b}$, and $\Delta\Delta G^\circ_{1.4e-1.4d}$ values are calculated to be -0.8 , -0.9 , and -0.6 kcal/mol, respectively, indicating that the substitution of one MeO group on a quinone ring leads to the favorable negative gain of ΔG° within $\Delta\Delta G^\circ = -0.6$ to -0.9 kcal/mol. In contrast, $\Delta\Delta G^\circ_{1.4d-1.4b}$ and $\Delta\Delta G^\circ_{1.4f-1.4e}$ are -1.6 and -1.7 kcal/mol, respectively. The negative gain of free energy change upon MeO substitution at the adjacent position is approximately 2 times larger than that of substitution at the separate position. The differential enthalpy changes, $\Delta\Delta H^\circ$,²⁴ show the same manner as the $\Delta\Delta G^\circ$ values; for example, $\Delta\Delta H^\circ_{1.4b-1.4a}$ and $\Delta\Delta H^\circ_{1.4d-1.4b}$ are -1.5 and -2.6 kcal/mol, respectively. Particularly, $\Delta\Delta H^\circ_{1.4d-1.4b}$ is about 2.4 times larger than $\Delta\Delta H^\circ_{1.4c-1.4b}$, although both 2,6-dimethoxy-*p*-benzoquinone (**4c**) and 2,3-dimethoxy-*p*-benzoquinone (**4d**) have two methoxy groups.^{9a} These data demonstrate that the affinities of **4a–f** depend on not only the number of MeO groups but also the position of MeO substituents bound to the quinone ring. The remarkable enhancement of binding affinity of **4d** compared with that of **4c** implies that the two adjacent MeO substituents at the 2- and 3-positions on the *p*-benzoquinone ring cooperatively act as the interaction site to form the bifurcated (three-center) hydrogen bonding, as shown in Scheme 3.²⁵ Furthermore, the extremely large entropy loss obtained in complexation between **1** and **4f** ($\Delta S^\circ_{1.4f} = -49.3$ eu) suggests that quinone **4f** is tightly fixed and that free rotation of four MeO groups about carbon (sp^2)–oxygen (MeO) bonds would be restricted on the porphyrin ring.

In contrast, there is no drastic change in the binding affinities for complexation between **2** and **4a–f** with the increase of the number of MeO substituents. Although the negative ΔH° values slightly increase by increasing the number of MeO substituents due to the electron-donating character of MeO groups, entropy changes upon binding are almost the same in the series of quinones. The differential free energy and enthalpy changes upon complexation for host **2** are quite different from those values for host **1** described above: $\Delta\Delta G^\circ_{2.4d-2.4b} = 0.2$ kcal/mol, $\Delta\Delta G^\circ_{(2.4f-2.4e)} = 0.4$ kcal/mol and $\Delta\Delta H^\circ_{2.4d-2.4b} = 0.2$ kcal/mol, $\Delta\Delta H^\circ_{2.4f-2.4e} = -0.7$ kcal/mol, respectively. These thermodynamic parameters indicate that two OH groups as functional sites in **2** interact with mainly two carbonyl groups of *p*-benzoquinone derivatives through two point hydrogen bonds. Thus, host porphyrin **2** has no ability to recognize the difference in the number and position of MeO groups, whereas the third and/or fourth OH groups in host porphyrin **1** play an important role of interaction with the adjacent two MeO substituents in **4d** and **4f**. The sharp difference in the binding properties between **1** and **2** is illustrated in Figure 4.

Table 2 indicates that the substitution of methyl group to the quinone ring is ineffective in the complexation between **1** and 2-methyl-*p*-benzoquinone (**4g**); for example, the differential free energy and enthalpy changes, $\Delta\Delta G^\circ_{1.4g-1.4a}$ and $\Delta\Delta H^\circ_{1.4g-1.4a}$,

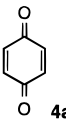
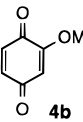
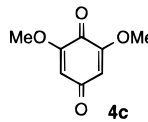
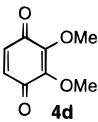
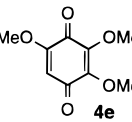
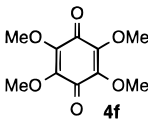
(22) Torsion angles about MeO groups are as follows: C(100)–O(12)–C(96)–C(91) = 175.5°, C(99)–O(11)–C(95)–C(96) = 111.7°, C(98)–O(9)–C(93)–C(94) = 166.9°, C(97)–O(8)–C(92)–C(93) = 121.4°, C(104)–O(13)–C(101)–C(102) = 77.8°, and C(105)–O(15)–C(103)–C(101) = -0.9° .

(23) The differential free energy change between **1·4b** and **1·4a** complexes are defined as follows: $\Delta\Delta G^\circ_{1.4b-1.4a} = \Delta G^\circ_{1.4b} - \Delta G^\circ_{1.4a}$.

(24) The differential enthalpy change between **1·4b** and **1·4a** complexes are defined as follows: $\Delta\Delta H^\circ_{1.4b-1.4a} = \Delta H^\circ_{1.4b} - \Delta H^\circ_{1.4a}$.

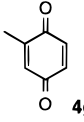
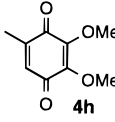
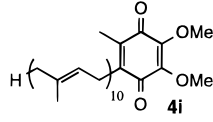
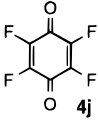
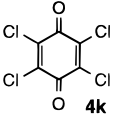
(25) Jeffrey, G. A.; Saenger, W. *Hydrogen Bonding in Biological Structures*; Springer-Verlag: Berlin, 1991; Chapter 8.

Table 1. Binding Constants and Thermodynamic Parameters for Porphyrin–Quinone Complex^a

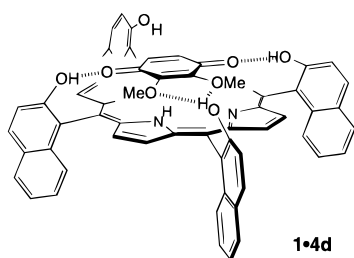
porphyrin	 4a	 4b	 4c	 4d	 4e	 4f	
1 (4 OHs)	K_a (M ⁻¹) ^b	(2.2 ± 0.1) × 10 ²	(8.6 ± 0.1) × 10 ²	(3.7 ± 0.1) × 10 ³	(1.3 ± 0.1) × 10 ⁴	(3.5 ± 0.1) × 10 ⁴	(6.1 ± 1.1) × 10 ⁵
	ΔH° (kcal/mol)	-8.1 ± 0.3	-9.6 ± 0.3	-10.7 ± 0.3	-12.2 ± 0.4	-14.0 ± 0.4	-22.7 ± 0.3
	$T\Delta S^\circ$ (kcal/mol) ^c	-4.9 ± 0.3	-5.5 ± 0.2	-5.9 ± 0.3	-6.7 ± 0.4	-7.8 ± 0.3	-14.7 ± 0.3
	ΔG° (kcal/mol) ^b	-3.2 ± 0.1	-4.0 ± 0.1	-4.9 ± 0.1	-5.6 ± 0.1	-6.2 ± 0.1	-7.9 ± 0.2
2 (2 OHs)	K_a (M ⁻¹) ^b	(9.8 ± 0.1) × 10	(3.2 ± 0.1) × 10 ²	(3.8 ± 0.3) × 10 ²	(2.2 ± 0.1) × 10 ²	(4.1 ± 0.1) × 10 ²	(2.1 ± 0.1) × 10 ²
	ΔH° (kcal/mol)	-7.1 ± 0.1	-8.5 ± 0.1	— ^d	-8.3 ± 0.2	-9.0 ± 0.5	-9.7 ± 0.3
	$T\Delta S^\circ$ (kcal/mol) ^c	-4.4 ± 0.1	-5.1 ± 0.1	— ^d	-5.1 ± 0.2	-5.4 ± 0.5	-6.5 ± 0.3
	ΔG° (kcal/mol) ^b	-2.7 ± 0.1	-3.4 ± 0.1	-3.5 ± 0.1	-3.2 ± 0.1	-3.6 ± 0.1	-3.2 ± 0.1

^a These parameters were determined in toluene in the range 278–323 K (five points). Enthalpy and entropy changes were calculated from van't Hoff plots. ^b At 298 K. ^c $T = 298$ K. ^d The solubility of **4c** is not sufficient for measurement of affinity at low temperature.

Table 2. Binding Constants and Thermodynamic Parameters for Porphyrin–Quinone Complex^a

porphyrin	 4g	 4h	 4i	 4j	 4k	
1 (4 OHs)	K_a (M ⁻¹) ^b	(2.0 ± 0.1) × 10 ²	(6.7 ± 0.1) × 10 ³	(1.7 ± 0.1) × 10 ³	(1.4 ± 0.1) × 10	(3.4 ± 0.1) × 10
	ΔH° (kcal/mol)	-8.2 ± 0.1	-11.5 ± 0.4	-10.2 ± 0.4	-4.6 ± 0.3	-6.1 ± 0.2
	$T\Delta S^\circ$ (kcal/mol) ^c	-5.0 ± 0.1	-6.3 ± 0.4	-5.8 ± 0.4	-3.0 ± 0.2	-4.1 ± 0.2
	ΔG° (kcal/mol) ^b	-3.1 ± 0.1	-5.2 ± 0.1	-4.4 ± 0.1	-1.6 ± 0.1	-2.1 ± 0.1
2 (2 OHs)	K_a (M ⁻¹) ^b	(1.6 ± 0.1) × 10 ²	(2.0 ± 0.1) × 10 ²	(1.3 ± 0.1) × 10 ²	(5.1 ± 0.1) × 10	(4.7 ± 0.3) × 10
	ΔH° (kcal/mol)	-7.9 ± 0.2	-8.5 ± 0.2	-8.6 ± 0.1	-6.4 ± 0.1	-9.9 ± 0.3
	$T\Delta S^\circ$ (kcal/mol) ^c	-4.9 ± 0.1	-5.3 ± 0.2	-5.7 ± 0.1	-4.0 ± 0.1	-7.7 ± 0.2
	ΔG° (kcal/mol) ^b	-3.0 ± 0.1	-3.1 ± 0.1	-2.9 ± 0.1	-2.3 ± 0.1	-2.3 ± 0.1

^a These parameters were determined in toluene in the range 278–323 K (five points). Enthalpy and entropy changes were calculated from van't Hoff plots. ^b At 298 K. ^c $T = 298$ K.

Scheme 3

are 0.1 and -0.1 kcal/mol, respectively. In contrast, the thermodynamic parameters of **2·4g** show more favorable values than those of **2·4a** ($\Delta\Delta H^\circ_{2\cdot4g-2\cdot4a} = -0.8$ kcal/mol). These differences suggest that the methyl group in **4g** may bring about steric hindrance to nonhydrogen-bonded OH groups in **1**, whereas there is no steric repulsion between **2** and **4g**. However, the binding affinity of 2,3-dimethoxy-6-methyl-*p*-benzoquinone (coenzyme Q₀) (**4h**) for **1** is quite larger than that of **4g**; $\Delta\Delta H^\circ_{1\cdot4h-1\cdot4g}$ and $\Delta\Delta G^\circ_{1\cdot4h-1\cdot4g}$ are determined to be -2.3 and -2.1 kcal/mol, respectively. The favorable thermodynamic parameters also imply the effective bifurcated hydrogen-bonding interaction between two adjacent MeO groups of **4h** and an OH group of **1**. Although native ubiquinone (coenzyme Q₁₀) (**4i**)

has a long isoprenoid chain and one methyl group which must bring about steric repulsion with a free OH group of **1**, sufficient affinity was observed due to the contribution of two adjacent MeO groups ($\Delta G^\circ_{1\cdot4i} = -4.4$ kcal/mol) to the binding event.

In a previous work, Aoyama and Ogoshi reported that electron deficient quinones such as fluoranil (**4j**) and chloranil (**4k**) interacted with a host porphyrin, 5,15-*cis*-bis(2-hydroxy-1-naphthyl)octaethylporphyrin (**3**), substituted with two hydroxynaphthyl groups at *meso*-positions and eight peripheral ethyl groups at β -positions of the porphyrin ring, via not only hydrogen bonding but also a charge-transfer-type interaction.^{8a,9a} The present host porphyrins, **1** and **2**, however, reveal poor affinities with **4j** and **4k**, as shown in Table 2. Thus, it is concluded that the driving force of complexation between a series of quinones and **1** or **2** is mainly due to the formation of multiple stable hydrogen bonds.

Enthalpy–Entropy Compensation Plot for Porphyrin–Quinone Complexes. It has been widely known that enthalpy–entropy compensation plots suggest the behavior of host–guest complexation and lead to the following empirical equation; $T\Delta S^\circ = \alpha\Delta H^\circ + T\Delta S^\circ_0$.²⁶ Using the data in Tables 1 and 2, plotting ΔH° against $T\Delta S^\circ$ at 298 K gives a good linear correlation with a coefficient of $r = 0.965$, as shown in Figure 5. The slope

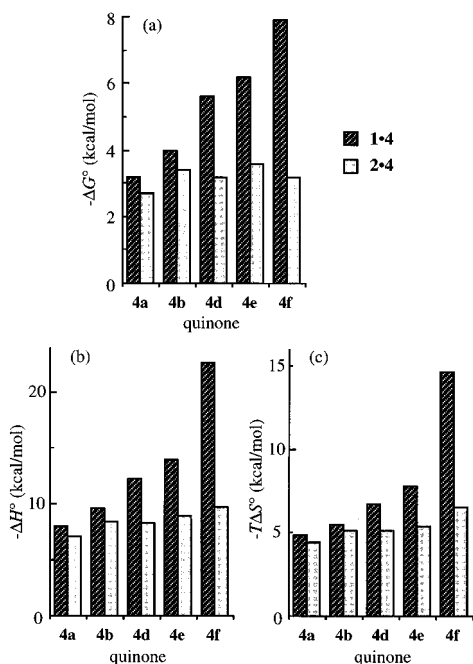


Figure 4. Comparison of thermodynamic parameters between **1·4** and **2·4** complexation in toluene at 298 K. (a) $-\Delta G^\circ$, (b) $-\Delta H^\circ$, and (c) $-T\Delta S^\circ$.

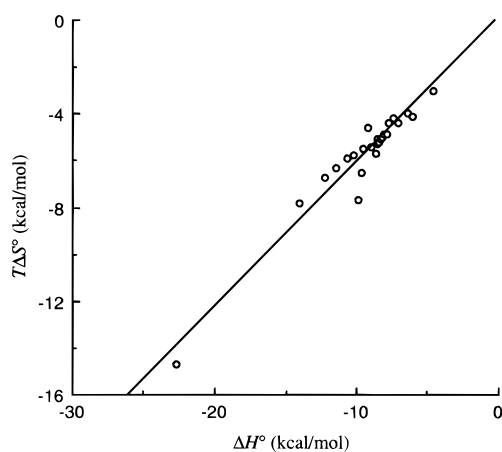


Figure 5. Enthalpy-entropy compensation plot for **1** and **2** with a series of **4** in toluene at 298 K. All plots in the graph refer to the entries in Tables 1 and 2.

(α) of the plot, which suggests the degree of conformational changes during complex formation, is 0.62 for the present system. The value is almost the same as that in the previous porphyrin **3**-quinone system or several metalloporphyrin-ligand ones.^{8a,27,28} The present α value indicates the minimal conformational change upon binding between quinone and porphyrin, compared to the reported values in previous studies.^{26c} This result suggests that the porphyrins **1** and **2** are preorganized host molecules for ubiquinone analogues, which is consistent with the result obtained from the NMR titration study or X-ray crystal structure analysis described above. Furthermore, compared with the previous data reported about the intercept of the

(26) (a) Inoue, Y.; Hakushi, T. *J. Chem. Soc. Parkin Trans. II*, **1985**, 935. (b) Inoue, Y.; Hakushi, T.; Liu, Y.; Tong, L.-H.; Shen, B.-J.; Jin, D.-S. *J. Am. Chem. Soc.* **1993**, *115*, 475. (c) Inoue, Y.; Liu, Y.; Tong, L.-H.; Shen, B.-J.; Jin, D.-S. *J. Am. Chem. Soc.* **1993**, *115*, 10637.

(27) Kuroda, Y.; Kato, Y.; Higashioji, T.; Hasegawa, J.; Kawanami, S.; Takahashi, M.; Shiraishi, N.; Tanabe, K.; Ogoshi, H. *J. Am. Chem. Soc.* **1995**, *117*, 10950.

(28) (a) Cole, S. J.; Curthoys, G. C.; Magnusson, E. A. *J. Am. Chem. Soc.* **1970**, *92*, 2991. (b) Kadish, K. M.; Schaeper, D. *J. Chem. Soc., Chem. Commun.* **1980**, 1273.

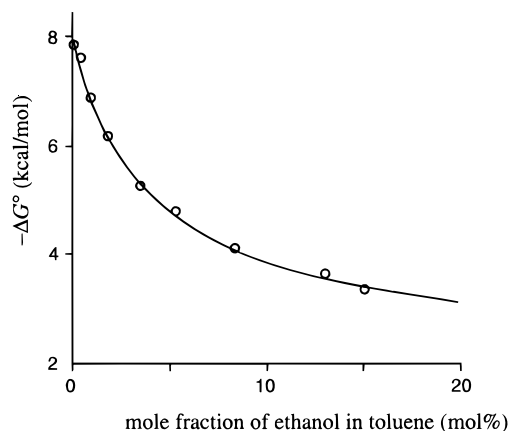


Figure 6. Dependence of ΔG° for **1·4f** complex formation on the solvent composition of toluene-ethanol mixtures at 298 K.

compensation plot, which is affected by solvation,^{26c} the present intercept value, $T\Delta S^\circ_0 = 0.11$ kcal/mol, is quite small. Therefore, according to a series of determined thermodynamic parameters, the present complexation is driven enthalpically, and the large negative enthalpy change due to the formation of multiple hydrogen bonding compensates for the unfavorable entropy loss derived from bimolecular association and the strict restraints on the rotation of MeO groups.

Solvent Effect on Hydrogen-Bonding Complexation. The large affinity observed in our model stimulated us to study the solvent effect on the binding behavior of the porphyrin-quinone adduct in solvents of different polarity controlled by the toluene-ethanol binary system. The binding constant and free energy change for the **1·4f** complex in the binary solvent were also determined from titrimetric measurement by UV-vis spectroscopy in a similar manner as above; (0–15 mol % of ethanol in toluene). Figure 6 shows the plots of affinities expressed by free energy changes (ΔG°) against the concentration of ethanol in toluene at 298 K. The decay of ΔG° in a nonlinear manner with the increase of cosolvent concentration suggests that ethanol weakens the affinity of **1·4f** complex through the functional group solvation in **1** and/or **4f**.

The NMR study of host **1** in the ethanol-toluene-*d*₈ binary system also supports that ethanol molecule(s) tightly interact with the OH groups in porphyrin **1**; Hydroxy protons at 4.97 ppm in toluene-*d*₈ shifted to downfield with the increase of concentration of ethanol and appeared at 5.78 ppm at 1.0 mol % of ethanol in toluene-*d*₈ at 298 K. Furthermore, the OH signals of **1** in the presence of ethanol shifted to downfield with a decrease in temperature; the chemical shifts of OH protons at 328, 298, and 278 K were 5.28, 5.83, and 6.65 ppm, respectively, in 1.1 mol % of ethanol in toluene. Therefore, the changes in chemical shift upon addition of ethanol indicate the temperature-dependent solvation in host **1** due to the multiple interactions between ethanol molecules and OH groups in **1**.

Determination of Heat Capacity Change for Host-Guest Complexation Formed by Hydrogen Bonding. To analyze the solvent effect on thermodynamic parameters for **1·4f** pairing, we further attempted to determine the affinity of **1** for **4f** at various concentrations of ethanol in toluene at 10–55 °C. The van't Hoff plots obtained from UV-vis titration measurements are illustrated in Figure 7. The plots in pure toluene display a linear relationship between $\ln K$ and $1/T$. The linear van't Hoff plots are also obtained in the presence of a higher concentration of ethanol (≥ 5.2 mol %) in toluene. In interesting contrast, the plots at 0.36–3.5 mol % of ethanol in toluene show a nonlinear relationship, suggesting that the enthalpy change

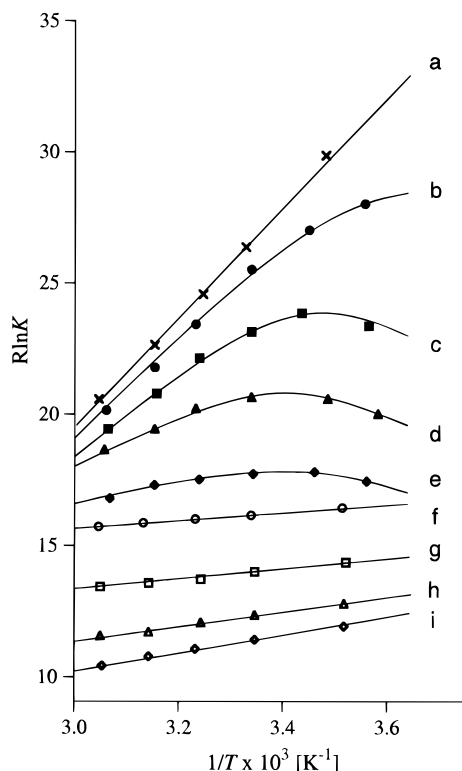


Figure 7. van't Hoff plots for the complexation between **1** and **4f** in the toluene-ethanol binary solvent. The mole fraction of ethanol (mol %) is as follows: (a) 0, (b) 0.36, (c) 0.90, (d) 1.8, (e) 3.5, (f) 5.2, (g) 8.3, (h) 13, and (i) 15. The best fit lines for a, f, g, h, and i are following $R \ln K = -\Delta H^\circ/T + \Delta S^\circ$. The best fit curves for c, d, and e are following eq 1. The curve for b is arbitrary.

Table 3. Thermodynamic Parameters, ΔG° , ΔH° , $T\Delta S^\circ$, and ΔC_p° , for **1**·**4f** Pairing Calculated from van't Hoff Plots at 298 K in Toluene-Ethanol Binary Solvent

mole fraction of ethanol (mol %) ^a	ΔG° ^{b,c}	ΔH° ^{b,c}	$T\Delta S^\circ$ ^{b,c}	ΔC_p° ^{d,e}
0	-7.9	-23	-15	0
0.90	-6.9	-6.2	0.77	-5.6×10^2
1.8	-6.1	-1.6	4.5	-4.0×10^2
3.5	-5.3	-0.57	4.7	-2.0×10^2

^a The thermodynamic parameters at 0.36 mol % ethanol in toluene are not shown here, since it is difficult to obtain accurate parameters due to the insufficient curvature of the van't Hoff plot. ^b Parameters are in kcal/mol. ^c Errors in ΔG° , ΔH° , and $T\Delta S^\circ$ are <5%. ^d Parameters are in cal/mol·K. ^e Errors in ΔC_p° are <10%.

(ΔH°) is the temperature-dependent term.²⁹ The variation of ΔH° with temperature is expressed in heat-capacity change upon complexation: $\Delta C_p^\circ = (\partial\Delta H^\circ/\partial T)_p$. By assuming that ΔC_p° is temperature independent in the range of present temperature, the magnitudes of ΔC_p° can be estimated from the degree of curvature in the van't Hoff plots:

$$R \ln K(T) = -(\Delta H^\circ(T)/T) + \Delta S^\circ(T) = -\{\Delta H^\circ(T_0) + (T - T_0)\Delta C_p^\circ\}/T + \Delta C_p^\circ \ln(T/T_0) + \Delta S^\circ(T_0) \quad (1)$$

where $K(T)$, $\Delta H^\circ(T)$, and $\Delta S^\circ(T)$ are temperature-dependent parameters and $\Delta H^\circ(T_0)$ and $\Delta S^\circ(T_0)$ are constants with $T = T_0$.³⁰ Table 3 depicts the thermodynamic parameters for **1**·**4f** complexation at 298 K. The obtained ΔC_p° parameters are

(29) Stauffer, D. A.; Barrans, R. E. Jr.; Dougherty, D. A. *J. Org. Chem.* **1990**, *55*, 2762.

(30) (a) Baldwin, R. L. *Proc. Natl. Acad. Sci. U.S.A.* **1986**, *83*, 8069. (b) Privalov, P. L.; Gill, S. J. *Adv. Protein Chem.* **1988**, *39*, 191.

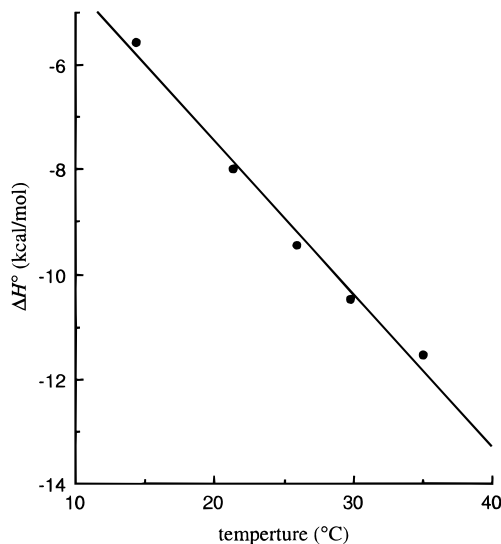


Figure 8. Enthalpy changes for **1**·**4f** complexation at 0.90 mol % ethanol in toluene as a function of temperature, $r = 0.993$.

negative and reach the maximum at 0.9 mol % of ethanol in toluene; $\Delta C_p^\circ = -5.6 \times 10^2$ cal/mol·K. In contrast, significant heat capacity changes for **1**·**4f** complexation were not observed in the toluene-2-butanone binary solvent.

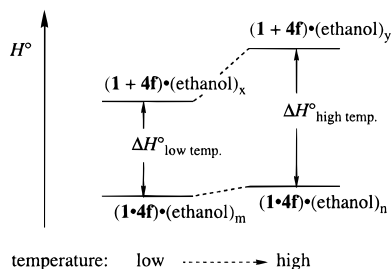
The heat (ΔH°) of **1**·**4f** complexation in toluene and toluene-ethanol binary solvent was also determined by microcalorimetric method.³¹ Figure 8 demonstrates that the ΔH° obtained by directly measuring the heat of complexation is largely temperature dependent in the presence of 0.9 mol % of ethanol in toluene. The large negative ΔC_p° for **1**·**4f** complexation is determined from the slope of Figure 8 to be approximately -3.0×10^2 cal/mol·K.^{32,33}

It is known that the change in heat-capacity term is one of the reliable parameters which shows the behavior of biological binding processes. For example, negative ΔC_p° arises from the temperature-dependent solvation of polar functional groups in protein and/or substrate, whereas positive ΔC_p° accompanies protein unfolding or dissolution of organic molecules in water.^{1b} Therefore, in our model system the large negative ΔC_p° is explained in terms of temperature variation in the degree of solvent-solute hydrogen bonding. In fact, NMR data clearly reveal that at lower temperature ethanol molecules tightly solvate OH groups in **1** and the degree of solvation seems to decrease with the increase of temperature. Scheme 4 illustrates a plausible mechanism of thermodynamic behavior, in which a negative change in the heat capacity ΔC_p° derives from the difference in ΔH° at different temperatures ($\Delta H^\circ = H^\circ_{\text{the state of the solvated complex 1·4f}} - H^\circ_{\text{the state of the solvated free 1 and 4f}}$, $\Delta H^\circ_{\text{low temp}} \neq \Delta H^\circ_{\text{high temp}}$ in Scheme 4). Assuming that the state of free **1** and **4f** is solvated more strongly than that of complex **1**·**4f**, the temperature-dependent changes in solvation of functional groups in free **1** and **4f** mainly dominate the magnitude of ΔH° .^{34b} Consequently, at lower concentration of ethanol cosolvent, a large negative ΔC_p° should be derived from

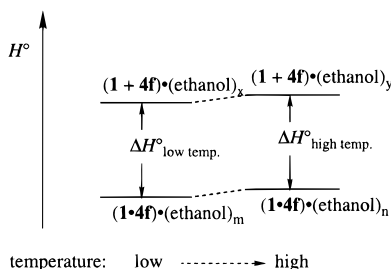
(31) Wiseman, T.; Williston, S.; Brandts, J. F.; Lin, L.-N. *Anal. Biochem.* **1989**, *179*, 131.

(32) We avoid further discussions on the determined value, since the stoichiometric value obtained from calorimetric measurement deviated from 1 (ca. $n = 0.9$), although the spectral data described above clearly show 1:1 complexation for **1** and **4f**.

(33) It is known that ΔC_p° also depends on temperature, $\Delta C_p^\circ(T) = \Delta C_p^\circ(T_0) + \alpha(T - T_0)$; however, the number of data points from Figure 8 was insufficient for curve-fitting analysis. Varadarajan, R.; Connely, P. R.; Sturtevant, J. M.; Richards, F. M. *Biochemistry* **1992**, *31*, 1421.

Scheme 4^a

^a condition: <5.2 mol % ethanol in toluene. $x > y$, $m \approx n$, $|\Delta H^\circ_{\text{low temp}}| < |\Delta H^\circ_{\text{high temp}}|$, $\Delta C_p^\circ < 0$.

Scheme 5^a

^a condition: >5.2 mol % ethanol in toluene. $x \approx y$, $m \approx n$, $|\Delta H^\circ_{\text{low temp}}| \approx |\Delta H^\circ_{\text{high temp}}|$, $\Delta C_p^\circ \approx 0$.

a rise in the enthalpy level of free **1** and **4f** due to the disruption of ethanol–solute hydrogen bonding with the increase of temperature (Scheme 4), whereas at higher concentration (≥ 5.2 mol %) ΔC_p° eventually approaches zero, since almost all the functional groups of free **1** and **4f** should be saturated by the excess amount of ethanol, even at high temperatures (Scheme 5). Thus, it is noted that the negative ΔC_p° associated with **1**•**4f** complexation can be detected in a *limited concentration range of ethanol cosolvent*.

In biological systems, a number of negative ΔC_p° values due to the association of ligand to protein have been reported. These values were determined in the range of -50 to -1000 cal/mol·K, deriving from the temperature-dependent ΔH° in terms of the hydrophobic contribution, hydrogen bonding, electrostatic interaction, and so on.^{1b} The thermodynamic changes obtained in biomolecules are the net result of all such interactions, and the dissection into these individual weak interactions seems to be difficult. To simplify the contribution of solvent effect to the stability of complex linked by hydrophobic interaction, several groups have recently presented the ΔC_p° values which derive from solvation of host and/or guest compounds in aqueous solvent ($\Delta C_p^\circ = -12$ to -190 cal/mol·K) by use of their model systems, such as cyclophane–arene complex and cyclodextrin–adamantane complex.^{29,34–36} In contrast, there are few reports which describe the quantitative ΔC_p° upon hydrogen-bonding complexation; Wilcox et al. have suggested that the heat capacity change upon diacid–aminopyrimidine complexation via hydrogen bonding is not significant in wet chloroform ($\Delta C_p^\circ < -30$ cal/mol·K).¹² Bonar-Law and Sanders have also shown the slightly bent van't Hoff plots for steroid-capped porphyrin–mannoside pairing related to hydrogen bonding in a mixture of tetrachloromethane and methanol; however, the degree of the curvature in the van't Hoff plots was too small to illuminate the thermodynamic aspects.¹¹ To

our knowledge, the present work in toluene–ethanol solution is the first example of such a large negative ΔC_p° (-5.6×10^2 cal/mol·K), showing that the magnitude of ΔC_p° depends on the concentration of ethanol cosolvent in the host–guest complexation formed by multiple hydrogen bonds.

Conclusions

Porphyrin **1** was designed as the first ubiquinone receptor to investigate ET reactions in the noncovalently linked porphyrin–quinone system. A series of thermodynamic and structural studies on **1**•**4** complexation shows that every OH group in **1** cooperatively acts as hydrogen-bonded sites not only for carbonyl groups but also for two adjacent MeO substituents bound to the ring of *p*-benzoquinone. Consequently, the ubiquinone analogues such as **4d–f** have large affinities with **1** via multiple hydrogen bonds. This study concludes that the four convergent OH groups in **1** are well-suited to stabilize the cofacial complexation between porphyrin and ubiquinone analogues.

Furthermore, we evaluated here the effect of polar solvent on thermodynamic parameters for the hydrogen-bonding interaction between **1** and **4f** in order to simulate the role of water in the hydrophobic binding pocket in an enzyme. In toluene–ethanol binary solvent, enthalpy changes upon complexation depend on temperature in a limited range of ethanol concentration in toluene due to the degree of the solvation of hydrogen-bonded sites in **1** and **4f**. This system led to a large negative heat capacity change upon binding at 0.9 mol % of ethanol in toluene; $\Delta C_p^\circ = -5.6 \times 10^2$ cal/mol·K.

In this work, we demonstrated that MeO substituents in ubiquinone can act as important hydrogen-bonded interaction sites in the specific molecular recognition process in protein.³⁷ Furthermore, using our model, we suggested here that solvation has crucial effect on the thermodynamic parameters for hydrogen-bond-based system in protein–ligand pairing. Finally, the present results indicate that porphyrin **1**–ubiquinone pairing is a suitable model to explore the specific binding behavior of ubiquinone to protein in hydrophobic lipid membrane.

Experimental Section

General Procedure. ¹H NMR spectra were recorded on JEOL A-500, GX-400 and FX-90Q spectrometers operated at 500, 400, and 90 MHz, respectively, and chemical shifts are reported relative to Me₄-Si at 0 ppm. ¹³C NMR spectra were recorded at 125 MHz on a JEOL A-500 spectrometer and ¹³C chemical shift is referenced to internal solvent chloroform (77.0 ppm). Mass spectra were recorded on a JEOL JMS-SX102A spectrometer. UV–visible spectra were recorded on a HITACHI U-3410 spectrophotometer and a Hewlett-Packard 8452A diode array spectrophotometer with a thermostated cell compartment controlled by a NESLAB circulation system. IR spectra were recorded on a Bio-Rad FTS-7 FT-IR spectrometer with a 4 cm⁻¹ resolution and a Parkin-Elmer System 2000 FTIR spectrometer with a 0.5 cm⁻¹ resolution. Toluene and ethanol were Dotite Spectrosol brand purchased from Dojindo Laboratories. Analytical thin-layer chromatography was performed with precoated Merck silica gel type 60, F₂₅₄.

Materials. *p*-Benzoquinone (**4a**) and 2-methyl-*p*-benzoquinone (**4g**) were purchased from Wako Pure Chemical Industries, Ltd. Methoxy-*p*-benzoquinone (**4b**) and 2,3-dimethoxy-6-methyl-*p*-benzoquinone (**4h**) were obtained from Tokyo Chemical Industry Co., Ltd. Tetrachloro-*p*-benzoquinone (**4k**) was purchased from Nacalai Tesque, Inc. Tetrafluoro-*p*-benzoquinone (**4j**) was obtained from Aldrich Chemical Co. Ubiquinone (**4i**) was purchased from Sigma Chemical Co. The quinones **4a**, **4b**, and **4g** were recrystallized before titration measure-

(34) (a) Smithrud, D. B.; Wyman, T. B.; Diederich, F. *J. Am. Chem. Soc.* **1991**, *113*, 5420. (b) Diederich, F.; Smithrud, D. B.; Sanford, E. M.; Wyman, T. B.; Ferguson, S. B.; Carcanague, D. R.; Chao, I.; Houk, K. N. *Acta Chem. Scand.* **1992**, *46*, 205.

(35) Harrison, J. C.; Eftink, M. R. *Biopolymers* **1982**, *21*, 1153.

(36) Zhang, B.; Breslow, R. *J. Am. Chem. Soc.* **1993**, *115*, 9353.

(37) (a) Sakamoto, K.; Miyoshi, H.; Matsushita, K.; Nakagawa, M.; Ikeda, J.; Ohshima, M.; Adachi, O.; Akagi, T.; Iwamura, H. *Eur. J. Biochem.* **1996**, *237*, 128. (b) Sakamoto, K.; Miyoshi, H.; Takegami, K.; Mogi, T.; Anraku, Y.; Iwamura, H. *J. Biol. Chem.* **1996**, *271*, 29897.

ment. 2,6-Dimethoxy-*p*-benzoquinone (**4c**),³⁸ 2,3-dimethoxy-*p*-benzoquinone (**4d**),³⁸ 2,3,5-trimethoxy-*p*-benzoquinone (**4e**),³⁹ and tetramethoxy-*p*-benzoquinone (**4f**)⁴⁰ were prepared by the previous literature method. Dipyrromethane (**6**),⁴¹ 5,15-diphenylporphyrin (**7**),¹⁵ and 5,15-dibromo-10,20-diphenylporphyrin (**8**)^{16,17b} were synthesized according to published procedures. 2-Methoxy-1-naphthaleneboronic acid (**9**) was prepared from 1-bromo-2-methoxynaphthalene and methyl borate.⁴²

meso-Tetrakis(2-methoxy-1-naphthyl)porphyrin (5). A 2-L round bottomed flask was charged with 2-methoxy-1-naphthaldehyde (3.72 g, 20.0 mmol), pyrrole (1.38 mL, 19.9 mmol), ethanol (15.0 mL), and benzene (2.0 mL). After the solution was purged with N₂ over 10 min, BF₃·OEt₂ (0.80 mL) was added via syringe and the mixture was stirred at room temperature for 12 h. After the addition of 2,3-dichloro-5,6-dicyano-1,4-benzoquinone (3.41 g, 15.0 mmol), the reaction mixture was further stirred at room temperature for 30 min. The solution was washed with water and the organic layer was dried over Na₂SO₄ and evaporated to dryness. The impurities were removed by column chromatography on silica gel (benzene–ethyl acetate, 10:1) to give a mixture of four atropisomers of *meso*-tetrakis(2-methoxy-1-naphthyl)porphyrin in 1.91 g (19.9%) yield.

meso-Tetrakis(2-hydroxy-1-naphthyl)porphyrin (1). A 300-mL round-bottomed flask fitted with a reflux condenser and a dropping funnel was charged with **5** (1.82 g, 1.95 mmol) in CH₂Cl₂ (300 mL). A 1.0 M BBr₃ solution in CH₂Cl₂ (30.0 mL) was added dropwise at 0 °C. After the solution was stirred at room temperature for 1.5 h, water (100 mL) was added to the reaction mixture, and the organic layer was washed with saturated NaHCO₃ (aq) (3 × 100 mL) and water (3 × 100 mL) and dried over Na₂SO₄. After evaporation, a mixture of four atropisomers of *meso*-tetrakis(2-hydroxy-1-naphthyl)porphyrin was obtained in 1.71 g (quant) yield.

meso-α,α,α,α-Tetrakis(2-hydroxy-1-naphthyl)porphyrin (1) was isolated from the atropisomeric mixture of *meso*-tetrakis(2-hydroxy-1-naphthyl)porphyrin (1.71 g) by column chromatography on silica gel (benzene–ethyl acetate = 1:1) in 0.178 g (10.4% based on the atropisomeric mixture) yield: TLC *R*_f = 0.24 (benzene–ethyl acetate = 1:1); ¹H NMR (CDCl₃, 500 MHz) δ 8.607 (8H, s), 8.205 (4H, d, *J* = 9.2 Hz), 8.013 (4H, d, *J* = 8.3 Hz), 7.571 (4H, d, *J* = 9.2 Hz), 7.319 (4H, dd, *J* = 8.3, 6.9 Hz), 7.063 (4H, dd, *J* = 8.5, 6.9 Hz), 6.890 (4H, d, *J* = 8.9 Hz), 4.903 (4H, s), –2.269 (2H, s); ¹³C NMR (CDCl₃, 125 MHz)⁴³ δ 154.27, 137.50, 131.25, 128.51, 127.75, 126.89, 126.69, 123.44, 119.99, 117.45, 110.94; UV–vis (CHCl₃) λ_{abs} (ε) 426 (1.71 × 10⁵), 516 (2.11 × 10⁴), 545 (3.69 × 10³), 587 (6.97 × 10³), 643 (6.73 × 10²) nm; HRMS (FAB) calcd for C₆₀H₃₈N₄O₄ (M⁺) 878.2893, found 878.2884.

5,15-Bis(2-methoxy-1-naphthyl)-10,20-diphenylporphyrin (10). A 100-mL round bottomed flask with a reflux condenser was charged with 5,15-dibromo-10,20-diphenylporphyrin (**8**), tetrakis(triphenylphosphine)palladium (0.15 g, 0.13 mmol), and benzene (80 mL). Solutions of 2-methoxy-1-naphthaleneboronic acid (**9**) (5.00 g, 24.7 mmol) and of Na₂CO₃ (aq) (2 M, 24.7 mL) in ethanol (15 mL) were added successively under nitrogen and the mixture was stirred at 80 °C for 12 h. After the reaction was completed, the reaction mixture was diluted with water (200 mL) and benzene (100 mL). The organic layer was separated, washed with water, and dried over MgSO₄. After evaporation to dryness, the obtained residue was purified by column chromatography on silica gel with hexane–benzene–ethyl acetate as eluent to give a mixture of *cis* and *trans* atropisomers of *meso*-tetrakis(2-methoxy-1-naphthyl)porphyrin in 1.50 g (90%) yield.

5,15-Bis(2-hydroxy-1-naphthyl)-10,20-diphenylporphyrin (2). A 500-mL round bottomed flask with a reflux condenser was charged with **10** (1.30 g, 1.68 mmol) in CH₂Cl₂ (500 mL). A 1.0 M BBr₃

solution in CH₂Cl₂ (30.0 mL) was added dropwise at 0 °C. After the solution was stirred at room temperature for 1.5 h, water (100 mL) was added to the reaction mixture, and the organic layer was washed with saturated NaHCO₃ (aq) (3 × 100 mL) and water (3 × 100 mL) and dried over Na₂SO₄. After evaporation, *cis* and *trans* atropisomers of 5,15-bis(2-hydroxy-1-naphthyl)-10,20-diphenylporphyrin were obtained in 1.25 g (quant) yield.

cis-5,15-Bis(2-hydroxy-1-naphthyl)porphyrin (**2**) was isolated from two isomers by column chromatography on silica gel (benzene–ethyl acetate = 10:1): TLC *R*_f = 0.39 (benzene–ethyl acetate = 10:1); ¹H NMR (CDCl₃, 500 MHz) δ 8.812 (4H, d, *J* = 4.9 Hz), 8.673 (4H, d, *J* = 4.8 Hz), 8.247 (2H, d, *J* = 9.2 Hz), 8.195 (2H, *J* = 7.0 Hz), 8.165 (2H, d, *J* = 7.7 Hz), 8.054 (2H, d, *J* = 7.9 Hz), 7.77–7.69 (6H, m), 7.629 (2H, d, *J* = 9.1 Hz), 7.343 (2H, ddd, *J* = 8.2, 6.7, 1.2 Hz), 7.034 (2H, ddd, *J* = 8.6, 6.7, 1.2 Hz), 6.845 (2H, d, *J* = 8.6 Hz), 5.001 (2H, s), –2.491 (2H, s); ¹³C NMR (CDCl₃, 125 MHz)⁴⁴ δ 154.22, 141.35, 137.66, 134.56, 134.44, 132.4 (br), 131.03, 130.8 (br), 128.53, 127.95, 127.72, 126.81, 126.78 (2C), 126.73, 123.37, 120.68, 120.66, 117.42, 110.00; UV–vis (CHCl₃) λ_{abs} (ε) 426 (1.71 × 10⁵), 516 (2.11 × 10⁴), 545 (3.69 × 10³), 587 (6.97 × 10³), 643 (6.73 × 10²) nm; UV–vis (toluene) λ_{abs} (ε) 423 (2.69 × 10⁵), 515 (1.99 × 10⁴), 548 (5.47 × 10³), 589 (5.87 × 10³), 645 (2.14 × 10³) nm; HRMS (FAB) calcd for C₅₂H₃₄N₄O₂ (M⁺) 746.2682, found 746.2700.

Determination of Binding Affinity from UV–Vis Titration.

Binding constants between porphyrin and quinone were determined by UV–vis spectrophotometric titration in toluene. A solution of host porphyrin (7.0 × 10^{−5} M, 2 mL) in toluene was poured into a 10-mm glass cell at 25 °C. Ten portions of a quinone solution were added successively to the solution of host porphyrin, and spectral change was monitored at 516 nm. The concentration of quinone solution was controlled by the binding affinity of porphyrin, in which about 80–90% of the porphyrin would be bound at the end of the titration. The parameters from the changes in monitored absorbance were calculated from nonlinear curve fitting analysis based on the damping Gauss–Newton method.

X-ray Structure Determination. A reddish-brown platelike crystal with dimensions of 0.1 × 0.2 × 0.2 mm³ was used for collection of diffraction intensities. Reflection data were obtained at 296 K with ω – 2θ scan mode on an Enraf Nonius CAD4-EXPRESS four-circle diffractometer using Cu Kα radiation (λ = 1.54178 Å) and a graphite monochromator. Crystal data and experimental details associated with data collection are reported in the Supporting Information. Data collection showed systematic absences (*h* + *l* = 2*n* + 1 for *h0l*), which led to two possible space groups, *Pn* and *P2/n*. The space group *P2/n* was tentatively assumed. The structure analysis is very difficult owing to too long a *c*-axis and too many parameters that are involved. The three standard reflections monitored every 2 h showed no significant variations. Reflection data were corrected for Lorentz and polarization effects. Absorption correction, based on a Ψ scan,⁴⁵ was applied for the crystal.

The structure was solved by the direct method using the SIR88 program.⁴⁶ The refinements were performed anisotropically for Cl, O, and N atoms and isotropically for C atoms, by full-matrix least-squares calculations, and the hydrogen atoms except for those of the methyl groups of **4f** were included as a fixed contribution in the least-squares, whose positions were idealized assuming a trigonal planar geometry and using a C–H length of 0.95 Å, since the ratio (no. of reflections)/(no. of variables) is small. Atomic scattering factors and anomalous dispersion terms were taken from the *International Tables for X-ray Crystallography IV*.⁴⁷ The *R* and *R*_w values were 0.15 and 0.21, respectively. The weighting scheme $w^{-1} = (\sigma^2(F_o) + (0.023F_o)^2)$ was employed for the crystal. The difference Fourier maps even at this stage did not show any significant features. In spite of repeated refinements, the reliability factors, unfortunately, did not converge to

(38) Orita, H.; Shimizu, M.; Hayakawa, T.; Takehira, K. *Bull. Chem. Soc. Jpn.* **1989**, *62*, 1652.

(39) Catlin, J. C.; Daves, D., Jr.; Folkers, K. *J. Med. Chem.* **1971**, *14*, 45.

(40) Akhtar, M. H.; Begleiter, A.; Johnson, D.; Lown, W.; McLaughlin, L.; Sim, S.-K. *Can. J. Chem.* **1975**, *53*, 2891.

(41) Chong, R.; Clezy, P. S.; Liepa, A. J.; Nichol, A. W. *Aust. J. Chem.* **1969**, *22*, 229.

(42) Washburn, R. M.; Levens, E.; Albright, C. F.; Billig, F. A. *Org. Synth.* **1963**, *39*, 3.

(43) C_α and C_β carbons of the four pyrrole rings were not detected due to the broadening derived from N–H tautomerism.

(44) C_α carbons of the four pyrrole rings were not detected due to the broadening derived from N–H tautomerism.

(45) North, A. C. T.; Phillips, D. C.; Mathews, F. S. *Acta Crystallogr., Sect. A*, **1968**, *24*, 351.

(46) Cascarano, G.; Giacovazzo, C.; Burla, M. C.; Polidori, G.; Camalli, M.; Spagna, R.; Viterbo, D. *SIR88*; University of Bari: Bari, Italy, 1988.

(47) Ibers, J. A.; Hamilton, W. C. *International Tables for X-ray Crystallography*; Kynoch: Birmingham, U.K., 1974; Vol. IV.

good values, which may attribute to incomplete peak separations due to the long *c*-axis. All calculations were carried out on a Micro VAX3100 and an IRIS Indigo XS-24 computer by using the program systems SDP-MolEN⁴⁸ and teXsan.⁴⁹

The crystal data, final positional parameters, bond lengths, and angles of the non-hydrogen atoms are listed in Supporting Information.

Calorimetric Titration. Calorimetric titration were performed in a adiabatic shield by using a MicroCal OMEGA calorimeter, which was connected to a microcomputer for the automatic titration and data processing. In a typical run, twenty portions ($5.0 \mu\text{L}$; $5.4 \times 10^{-3} \text{ M}$) of **4f** were introduced into 1.35 mL of solution of **1** ($2.0 \times 10^{-4} \text{ M}$) intermittently at intervals of 3 min. Each portion was introduced during the course of 15 s. A titration curve was obtained by plotting the calorific value against the amount of **4f**, from which the binding constant and the enthalpy change of formation of **1**·**4f** pair were calculated. The heat of dilution of **4f** was measured separately, for which no significant calorific value was detected.

(48) SDP-MolEN: An Interactive Structure Solution Procedure; Enraf-Nonius: Delft, The Netherlands, 1990.

(49) teXsan: Crystal Structure Analysis Package, Molecular Structure Corp., 1985, 1992.

Acknowledgment. This work was supported by a Grant-in-Aid for Specially Promoted Research (no. 04101003) from the Ministry of Education, Science, and Culture, Japan. We are grateful to Dr. M. Takagi and Dr. T. Ihara, Kyushu University, for the measurement of calorimetry. We would like to thank Prof. C. Wilcox, University of Pittsburgh, for many valuable discussions concerning the solvent effect on host-guest interaction. We appreciate the helpful suggestion from Dr. J. Brandts, Microcal Inc. T.H. also acknowledges partial support of this work by the Hattori Hoko-kai Foundation.

Supporting Information Available: ¹H and ¹³C spectra for **1** and **2**, IR spectral data for **1**, **4f**, and the **1**·**4f** complex, and crystallographic data with complete tables of positional parameters, bond distances and angles, torsion angles, displacement parameters, and the view of another half-independent molecule of **1**·**4f** pair in the unit cell (27 pages). See any current masthead page for ordering and Internet access instructions.

JA9711526